Boundary Integral Approach to the Scattering of Nonplanar Acoustic Waves by Rigid Bodies

Judith M. Gallman*
NASA Ames Research Center, Moffett Field, California 94035
M. K. Myers†
George Washington University, Hampton, Virginia 23665
and
F. Farassat‡
NASA Langley Research Center, Hampton, Virginia 23665

The acoustic scattering of an incident wave by a rigid body can be described by a singular Fredholm integral equation of the second kind. This equation is derived by solving the wave equation using generalized function theory, Green's function for the wave equation in unbounded space, and the acoustic boundary condition for a perfectly rigid body. This paper discusses the derivation of the wave equation, its reformulation as a boundary integral equation, and the solution of the integral equation by the Galerkin method. The accuracy of the Galerkin method can be assessed by applying the technique outlined in the paper to reproduce the known pressure fields that are due to various point sources. From the analysis of these simpler cases, the accuracy of the Galerkin solution can be inferred for the scattered pressure field caused by the incidence of a dipole field on a rigid sphere. The solution by the Galerkin technique can then be applied to such problems as a dipole model of a propeller whose pressure field is incident on a rigid cylinder. This is the groundwork for modeling the scattering of rotating blade noise by airplane fuselages.

Nomenclature

c = speed of propagation of sound
c_i = unknown coefficients in Eq. (18)
d_i = unknown coefficients in Eq. (18)
F_1, F_2 = defined by Eq. (23)
$f(\boldsymbol{x}) = 0$ = equation of the surface S
K_1, K_2 = kernel functions
k = wave number
$\boldsymbol{l}$ = dipole moment
$\boldsymbol{n}$ = unit outward surface normal
p_d = pressure field caused by a point dipole
$p_{d,n}$ = normal derivative of p_d
p_i = incident pressure field
p_m = pressure field caused by a point monopole
$p_{m,n}$ = normal derivative of p_m
p_s = scattered pressure field
$p_{s,n}$ = normal derivative of p_s
Q = monopole source strength
R = $|\boldsymbol{y} - \boldsymbol{X}|$
r = $|\boldsymbol{x} - \boldsymbol{y}|$, the distance between the observer and the source
S = surface described by $f(\boldsymbol{x}) = 0$
$S_i(\boldsymbol{x})$ = defined by Eq. (22a)
$T_i(\boldsymbol{x})$ = defined by Eq. (22b)
t = observer time
$\boldsymbol{X}$ = location of the acoustic source
$\boldsymbol{x}$ = observer point
$\boldsymbol{y}$ = source point
α = source azimuthal angle in spherical coordinates
γ = source polar angle in spherical coordinates
Θ = observer polar angle in spherical coordinates
θ = angle between the radiation vector and the unit normal to the surface
ρ = radial distance in spherical coordinates
τ = source time
τ^* = retarded time, $\tau^* = t - r/c$
ϕ = observer azimuthal angle in spherical coordinates
Ψ_i = basis functions
ω = angular frequency

Operators

$\delta(\cdot)$ = Dirac delta function
$\Box^2$ = wave operator
$\bar{\Box}^2$ = generalized wave operator in which the space and time derivatives are in the sense of distributions (generalized derivatives)

Received Aug. 31, 1990; presented as Paper 90-3945 at the AIAA 13th Aeroacoustics Conference, Tallahassee, FL, Oct. 22–24, 1990; revision received March 19, 1991; accepted for publication June 3, 1991.

*Research Scientist, U.S. Army Aeroflightdynamics Directorate. Member AIAA.
†Professor, Joint Institute for Advancement of Flight Sciences. Associate Fellow AIAA.
‡Senior Research Scientist. Associate Fellow AIAA.

Introduction

ONE goal in the development of noise prediction procedures for advanced turboprops is the development of a code that will predict fuselage scattering. The present work is intended to be a first step toward that goal; its object is to develop efficient and accurate numerical techniques for application to scattering problems.

A scattering problem is defined as the interaction between an obstacle with prescribed surface boundary conditions, such as the fuselage, and an incident wave field, which could be the acoustic pressure from the advanced turboprop.[1] Previous work on acoustic scattering problems that can be applied to the goal of this work has been concerned mainly with time-harmonic plane waves that approach from infinity and impinge on spherical or cylindrical objects or on surfaces with sharp discontinuities.[2] The classical approach is to solve the wave equation using the separation-of-variables technique, in which the incident plane wave is expressed in curvilinear coordinates appropriate to the scattering object. The scattered wave, which is the difference between the actual wave and the wave that would be present if the scattering obstacle were absent, is determined by applying the surface boundary conditions to find the appropriate constants in the separation-of-variables solution.[3] This results in a series solution that does not lend itself well to analysis, except in the far field, and is expensive to calculate with numerical accuracy. In addition, the separation-of-variables method applies only to the scattering surfaces of a few special shapes or geometries.

More recently, the boundary integral approach has been applied to the scattering of plane time-harmonic waves.[4] This approach reformulates the wave equation into an equivalent boundary integral equation that can be solved approximately for any scattering surface. By using techniques such as the Galerkin method, the integral equation can be reduced to a linear system of algebraic equations.

The first step toward the prediction of fuselage scattering, and the subject of the current work, is to apply the boundary integral approach to the scattering of time-harmonic, nonplanar acoustic waves incident on rigid bodies. The approach is to formulate the scattered pressure field as a homogeneous wave equation in the region exterior to the scattering surface and to incorporate the incident wave field in the boundary condition on the scattering surface. Then, by the use of generalized function theory, a wave equation for the scattered pressure field can be obtained that is valid over all of three-dimensional space. The scattered pressure field solution is then written as an integral equation through the utilization of the free-space Green's function for the wave equation. This resulting integral equation is Kirchhoff's representation of the scattered pressure field.

If a suitable distribution of sources, in this case the scattered surface pressure, is known, the scattered pressure throughout the field can be determined from the Kirchhoff representation.[5] A singular Fredholm integral equation of the second kind, which is solved for the scattered surface pressure, results from Kirchhoff's representation when the field point is taken to be on the scattering surface. The rigid-body boundary condition, defined on the scattering surface and containing information about the known incident wave field, is incorporated directly into this boundary integral equation.[6] This solution for the scattered surface pressure can be used in Kirchhoff's representation to find the scattered pressure at any point exterior to the scattering object.

This work contains a brief discussion of the derivation of Kirchhoff's representation for the scattered pressure field and a solution by the Galerkin method of the boundary integral equation that results from Kirchhoff's representation when the field point is on the surface. In order to prove that the formulation of the boundary integral equation and its solution by the Galerkin method is feasible, the same approach is applied to the Kirchhoff representation of the point monopole and point dipole pressure fields, which have exact solutions. After the formulation of the boundary integral equation and its solution by the Galerkin method is deemed feasible, another test is run to establish certainty about the scattered pressure solution. The monopole source is placed in the far field and its pressure field is allowed to scatter off a rigid sphere. The scattered pressure, obtained via the Galerkin method, is compared to the separation-of-variables solution for the scattering of plane waves by a rigid sphere.

Theory

Acoustic wave propagation is governed by the wave equation that is obtained by linearizing, via small-perturbation theory, the ideal-fluid equations of motion. A pressure field is said to satisfy the wave equation when

$$\Box^2 p = \frac{1}{c^2}\frac{\partial^2 p}{\partial t^2} - \nabla^2 p = Z(\boldsymbol{x},t) \tag{1}$$

where c is the speed of propagation of sound in the ambient fluid medium, and $Z(\boldsymbol{x},t)$ is an inhomogeneous term representing the source of the acoustic disturbance. The acoustic boundary condition for a rigid surface S, which is described by $f(\boldsymbol{x}) = 0$ where $f > 0$ exterior to S, is

$$p_n = \frac{\partial p}{\partial n} = 0 \qquad \text{on } S \tag{2}$$

The causality condition ensures that the pressure waves are outgoing as $|\boldsymbol{x}|$ approaches infinity, and it must also be satisfied.

The pressure field p can be expressed as the sum of an incident field and the scattered pressure field in the form

$$p = p_i + p_s \tag{3}$$

in which p_i is defined so that it satisfies

$$\Box^2 p_i(\boldsymbol{x},t) = Z(\boldsymbol{x},t) \tag{4}$$

This requires that p_s satisfy the homogeneous wave equation in the region where $f > 0$

$$\Box^2 p_s(\boldsymbol{x},t) = 0 \tag{5}$$

The boundary condition of Eq. (2) becomes

$$\frac{\partial p_s}{\partial n} = -\frac{\partial p_i}{\partial n} \qquad \text{on } S \tag{6}$$

Derivation of Kirchhoff's Formula for the Scattered Pressure Field

The source of the acoustic disturbance, or the incident pressure field, is known and can be used in the boundary condition of Eq. (6) along with the application of Kirchhoff's formula to solve for the scattered pressure field. A brief description of the derivation of Kirchhoff's formula is presented here.

Define $\hat{P}_s$ over the entire three-dimensional space by

$$\hat{P}_s(\boldsymbol{x},t) = \begin{cases} p_s(\boldsymbol{x},t) & f > 0 \\ 0 & f < 0 \end{cases} \tag{7}$$

This implies that there exists a jump discontinuity in $\hat{P}_s$ across the surface $f(\boldsymbol{x}) = 0$ whose magnitude is equal to the value of the scattered pressure on the surface. From generalized function theory and Ref. 7, the generalized d'Alembertian of $\hat{P}_s$ is

$$\bar{\Box}^2 \hat{P}_s = \Box^2 p_s - p_{s,n}\,\delta(f) - \bar{\nabla}\cdot[p_s \boldsymbol{n}\,\delta(f)] \tag{8}$$

where the bar over the operator indicates a generalized derivative.[8-10] The ordinary d'Alembertian in the region where the derivatives of the scattered pressure field are defined is equal to zero by Eq. (5) when $f > 0$ and by Eq. (7) when $f < 0$. Therefore, Eq. (8) becomes

$$\bar{\Box}^2 \hat{P}_s = -p_{s,n}\,\delta(f) - \bar{\nabla}\cdot[p_s \boldsymbol{n}\,\delta(f)] \tag{9}$$

Since Eq. (9) holds over all space, the free-space Green's function for the wave equation can be utilized to find the solution for the scattered pressure field! The free-space Green's function is

$$G(\boldsymbol{x},t;\,\boldsymbol{y},\tau) = \begin{cases} \dfrac{\delta(g)}{4\pi r} & t \geq \tau \\ 0 & t < \tau \end{cases} \tag{10}$$

Here $r = |\boldsymbol{x} - \boldsymbol{y}|$ is the distance between the observer point and the source point, and $g = t - (\tau + r/c)$ is the equation of the collapsing sphere centered at the observer point. The use of the Green's function of Eq. (10) ensures that the causality condition for the pressure field is satisfied. Using Eq. (9) and the Green's function, the solution for the scattered pressure field is expressed in the form

$$4\pi\hat{P}_s = -\int_{-\infty}^{t}\int_{-\infty}^{\infty} p_{s,n}(y,\tau)\,\delta(f)\,\frac{\partial(g)}{r}\,\mathrm{d}y\,\mathrm{d}\tau - \overline{\nabla}\cdot\int_{-\infty}^{t}\int_{-\infty}^{\infty} p_s(y,\tau)\boldsymbol{n}\,\delta(f)\,\frac{\delta(g)}{r}\,\mathrm{d}y\,\mathrm{d}\tau \tag{11}$$

where the inner integral is over the entire unbounded three-dimensional space.

The τ integration in Eq. (11) is simple when it is performed by changing the variable of integration to g, the Jacobian of the transformation $|\partial\tau/\partial g|$ being unity. This integration restricts the remaining terms in the integral to $g = 0$, introducing the retarded time $\tau^* = t - r/c$. The integration over y results in a surface integral because of the Dirac delta function of f

$$4\pi\hat{P}_s(x,t) = -\int_{f=0}\frac{1}{r}\,p_{s,n}(y,\tau^*)\mathrm{d}S - \overline{\nabla}\cdot\int_{f=0}\frac{1}{r}\,\boldsymbol{n}p_s(y,\tau^*)\mathrm{d}S \tag{12}$$

Now the divergence operator is brought inside the second integral, which yields

$$4\pi\hat{P}_s(x,t) = -\int_{f=0}\frac{1}{r}\,p_{s,n}(y,\tau^*)\mathrm{d}S + \int_{f=0}\left(\frac{\cos\theta}{r^2}\,p_s(y,\tau^*) + \frac{\cos\theta}{rc}\frac{\partial}{\partial t}p_s(y,\tau^*)\right)\mathrm{d}S \tag{13}$$

Here $\cos\theta$ is the scalar product of the outward-pointing unit normal and the radiation-direction unit vector, $(x - y)/r$. Equation (13) is the Kirchhoff representation of the scattered pressure field. By definition, the Kirchhoff representation requires information about the pressure on the surface of integration. If the observer is assumed to be on the surface, the Kirchhoff representation can be solved as a boundary integral equation for the surface pressure. Once the surface pressure is known, the determination of the scattered pressure at any point in the field is reduced to a numerical integration using Eq. (13) again. The total pressure field for $f > 0$ is the sum of the incident and scattered pressure fields.

When the observer point lies on the surface S, then, as shown in Ref. 14, Appendix A, Eq. (13) becomes

$$2\pi\hat{P}_s(x,t) = -\int_{f=0}\frac{1}{r}\,p_{s,n}(y,\tau^*)\mathrm{d}S + \int_{f=0}\left(\frac{\cos\theta}{r^2}\,p_s(y,\tau^*) + \frac{\cos\theta}{rc}\frac{\partial}{\partial t}p_s(y,\tau^*)\right)\mathrm{d}S \tag{14}$$

Note that when the observer point and the source point coincide, the integrands in Eq. (14) are singular. Hence, it is labeled as a singular Fredholm integral equation of the second kind.

In the current work, since the incident pressure field is taken to be harmonic in time, the scattered pressure field is assumed to be time harmonic. Therefore, the scattered pressure field on the surface S can be expressed as

$$p_s(x,t) = A(x)\cos\omega t + B(x)\sin\omega t \tag{15}$$

where ω is the angular frequency.

Substituting Eq. (15) and its partial time derivative into Eq. (14) yields

$$2\pi(A(x)\cos\omega t + B(x)\sin\omega t) = -\int_{f=0}\frac{1}{r}p_{s,n}(y,\tau^*)\mathrm{d}S + \int_{f=0}\frac{\cos\theta}{r^2}[A(y)(\cos\omega\tau^* - kr\sin\omega\tau^*) + B(y)(\sin\omega\tau^* + kr\cos\omega\tau^*)]\mathrm{d}S \tag{16}$$

where k is the wave number and is equal to ω/c. In the current work, Eq. (16), with $p_{s,n}$ found from the boundary condition in Eq. (6), is solved for $A(x)$ and $B(x)$ by use of the Galerkin method. This method is presented in the next section.

Solution by Galerkin Method

The Galerkin method, also known as the method of weighted residuals, proceeds by forcing a residual to be orthogonal to a set of weighting functions.[12] The residual in this case is defined to be

$$R(x,t) = 2\pi(A(x)\cos\omega t + B(x)\sin\omega t) + \int_{f=0}\frac{1}{r}\,p_{s,n}(y,\tau^*)\mathrm{d}S - \int_{f=0}\frac{\cos\theta}{r^2}\,[A(y)(\cos\omega\tau^* - kr\sin\omega\tau^*) + B(y)(\sin\omega\tau^* + kr\cos\omega\tau^*)]\mathrm{d}S \tag{17}$$

so that $R(x,t)$ is a measure of the error by which an assumed solution fails to satisfy Eq. (17). The weighting functions are chosen to be equal to the basis functions, or approximating functions, which must be a linearly independent set of functions for the approximation to be meaningful. If the basis functions are denoted as $\Psi_i(x)$, then the unknown functions are assumed to be given by

$$A(x) \approx \sum_{i=1}^{N} c_i\,\Psi_i(x), \quad B(x) \approx \sum_{i=1}^{N} d_i\,\Psi_i(x) \tag{18}$$

The definition of the basis functions usually, but not necessarily, depends on the geometry of the problem, or in this case, that of the scattering object. If the basis functions are chosen from a complete set of functions (which guarantees linear independence), then the approximation in Eq. (18) becomes exact as N approaches infinity. To satisfy completeness, one can take as the basis functions the eigenfunctions of a related homogeneous boundary value problem. For example, in spherical coordinates the basis functions would be a complete set of Legendre or associated Legendre polynomials.

As defined previously, $\tau^* = t - r/c$, so that $\omega\tau^* = \omega t - kr$. Let $\omega t = 0$ so that Eq. (17) becomes

$$R_1(x) = 2\pi A(x) + \int_{f=0}\frac{1}{r}\,[p_{s,n}(y,\tau^*)]_{\omega t=0}\,\mathrm{d}S - \int_{f=0}\frac{\cos\theta}{r^2}\,[A(y)\,(kr\sin kr + \cos kr) + B(y)(kr\cos kr - \sin kr)]\mathrm{d}S \tag{19}$$

Then let $\omega t = \pi/2$, and the second form of the residual becomes

$$R_2(x) = 2\pi B(x) + \int_{f=0}\frac{1}{r}\,[p_{s,n}(y,\tau^*)]_{\omega t=\pi/2}\,\mathrm{d}S + \int_{f=0}\frac{\cos\theta}{r^2}\,[A(y)(kr\cos kr - \sin kr) - B(y)(kr\sin kr + \cos kr)]\mathrm{d}S \tag{20}$$

For convenience and clarity, define the kernels to be

$$K_1(x;y) = kr\sin kr + \cos kr \tag{21a}$$

$$K_2(x;y) = kr\cos kr - \sin kr \tag{21b}$$

These kernels, along with the assumed solutions in Eq. (18), can be used to express those integrals in the residuals that contain the unknown functions as

$$S_i(x) = \int_{f=0} \frac{\cos\theta}{r^2} \Psi_i(y) K_1(x;y) \mathrm{d}S \tag{22a}$$

$$T_i(x) = \int_{f=0} \frac{\cos\theta}{r^2} \Psi_i(y) K_2(x;y) \mathrm{d}S \tag{22b}$$

For further convenience in notation, define

$$F_1(x) = \int_{f=0} \frac{1}{r} [p_{s,n}(y,\tau^*)]_{\omega t=0} \, \mathrm{d}S \tag{23a}$$

$$F_2(x) = \int_{f=0} \frac{1}{r} [p_{s,n}(y,\tau^*)]_{\omega t=\frac{\pi}{2}} \, \mathrm{d}S \tag{23b}$$

Here F_1 and F_2 consist of the direct application of the boundary information that is determined by the incident wave field. Using the definitions from Eqs. (21), (22), and (23), the residuals can be simply written in the forms

$$R_1(x) = \sum_{i=1}^{N} c_i[2\pi\Psi_i(x) - S_i(x)] - \sum_{i=1}^{N} d_i T_i(x) + F_1(x) \tag{24a}$$

$$R_2(x) = \sum_{i=1}^{N} d_i[2\pi\Psi_i(x) - S_i(x)] + \sum_{i=1}^{N} c_i T_i(x) + F_2(x) \tag{24b}$$

The orthogonality conditions that are required between the residual and the weighting functions are

$$\int_{f=0} R_1(x)\, \Psi_j(x) \mathrm{d}S = 0 \quad j = 1, N \tag{25a}$$

$$\int_{f=0} R_2(x)\, \Psi_j(x) \mathrm{d}S = 0 \quad j = 1, N \tag{25b}$$

The application of these last two conditions to the expressions in Eq. (24) results in a linear system of $2N$ algebraic equations in $2N$ unknowns, in the form

$$-\int_{f=0} \Psi_j(x) F_1(x) \mathrm{d}S = \sum_{i=1}^{N} c_i \int_{f=0} \Psi_j(x)[2\pi\Psi_i(x) - S_i(x)]\mathrm{d}S - \sum_{i=1}^{N} d_i \int_{f=0} \Psi_j(x) T_i(x) \mathrm{d}S \quad j = 1, N \tag{26a}$$

$$-\int_{f=0} \Psi_j(x) F_2(x) \mathrm{d}S = \sum_{i=1}^{N} d_i \int_{f=0} \Psi_j(x)\,[2\pi\Psi_i(x) - S_i(x)]\mathrm{d}S + \sum_{i=1}^{N} c_i \int_{f=0} \Psi_j(x) T_i(x) \mathrm{d}S \quad j = 1, N \tag{26b}$$

Finally, this linear system of algebraic equations is solved for the coefficients c_i and d_i; the scattered pressure field on the surface $f = 0$ is then known and takes the form

$$p_s(x,t) = \sum_{i=1}^{N} c_i \Psi_i(x) \cos\omega t + \sum_{i=1}^{N} d_i \Psi_i(x) \sin\omega t \tag{27}$$

Total Acoustic Pressure Field

The solution for the scattered pressure on the surface $f = 0$ and its partial derivative with respect to time, when incorporated into the Kirchhoff representation in Eq. (13), yield the scattered pressure for any point in the field $f > 0$. After the substitution of Eq. (27), its partial derivative with respect to time, and the boundary condition of Eq. (6) into Eq. (13), the expression for the scattered pressure field is

$$4\pi\hat{P}_s(x,t) = \int_{f=0} \frac{1}{r} \frac{\partial}{\partial n} p_i(y,\tau^*) \mathrm{d}S + \int_{f=0} \frac{\cos\theta}{r^2} \sum_{i=1}^{N} [c_i \Psi_i(y)(\cos\omega\tau^* - kr\sin\omega\tau^*) + d_i \Psi_i(y)(\sin\omega\tau^* + kr\cos\omega\tau^*)]\mathrm{d}S \tag{28}$$

Equation (28) is applicable to any rigid scattering surface and any time-harmonic incident pressure field that satisfies the wave equation.

As shown in Eq. (3), the total pressure is the sum of the incident and scattered pressure fields. The accuracy of the total acoustic pressure field depends on the accuracy of the scattered surface pressure solution obtained by using the Galerkin method as described in the previous section of the current work. Since there are very few known analytical solutions for the scattering of nonplanar, time-harmonic waves, there is no simple way to assess the accuracy of the scattered surface pressure as predicted by Eq. (28). To gain confidence that the scattered surface pressure is correct, the Galerkin method will be tested in some detail in the work that follows by assuming an unknown function for the surface distribution in the Kirchhoff representations of the point-source fields, as was done for the scattered pressure field. The Galerkin method solution for the point-source fields can then be compared to the exact solution and its accuracy can be verified.

Galerkin Method for Point-Source Pressure Fields

The unknown function that describes the surface distribution in the Kirchhoff representation is assumed to be harmonic and of the form

$$p|_{f=0}(x,t) = A(x)\cos\omega t + B(x)\sin\omega t \tag{29}$$

The unknown functions, $A(x)$ and $B(x)$, are defined in terms of the basis functions in Eq. (18). The surface over which the distribution is sought is spherical since this is the simplest case. The basis functions are Legendre polynomials or associated Legendre polynomials, depending on the symmetry of the pressure field. The monopole and certain orientations of the dipole, when placed inside the sphere, are axially symmetric with respect to the x_3 axis and are independent of the azimuth angle. These cases will be determined from basis functions that are Legendre polynomials. Other dipole orientations result in pressure fields that are not axially symmetric with respect to the x_3 axis and are functions of both the spherical azimuthal and polar angles. However, these pressure fields are even functions of the azimuthal angle, so the basis functions will be chosen as $\cos m\phi P_n^m(\cos\Theta)$.

The only differences between the Galerkin methods for scattered pressure fields and for point-source pressure fields are the definitions of the functions $F_1(x)$ and $F_2(x)$, which are defined for scattered pressure in Eq. (23). For the monopole field these functions are defined as

$$F_1(x) = \int_0^{2\pi}\int_0^{\pi} \frac{(\rho\cos\gamma - a)}{4\pi r R^3} [\cos k(r + R) + kR\sin k(r + R)]a^2 \sin\gamma \mathrm{d}\gamma \mathrm{d}\alpha \tag{30a}$$

$$F_2(x) = \int_0^{2\pi}\int_0^{\pi} \frac{(\rho\cos\gamma - a)}{4\pi r R^3} [\sin k(r + R) - kR\cos k(r + R)]a^2 \sin\gamma \mathrm{d}\gamma \mathrm{d}\alpha \tag{30b}$$

Here $p_{s,n}$ has been replaced with $p_{m,n}$, where

$$p_m(\boldsymbol{x},t) = \frac{Q}{4\pi R}\cos(kR - \omega t) \tag{31}$$

The monopole source strength is given by $Q = 1$, and the point source is located at $\boldsymbol{X} = \rho \boldsymbol{e}_3$, where $0 \leq \rho < a$ and a is the radius of the sphere. Inside the integral, R is defined as $|\boldsymbol{y} - \boldsymbol{X}|$ and for the spherical surface is

$$R = [a^2 + \rho^2 - 2\rho a \cos\gamma]^{1/2} \tag{32}$$

Figure 1 shows the geometry for a dipole source both inside and outside the spherical surface with the observer on the surface. For the dipole pressure field, $p_{s,n}$ is replaced with $p_{d,n}$, where

$$p_d(\boldsymbol{x},t) = \frac{l_i R_i}{4\pi R^3}[kR\sin(\omega t - kR) - \cos(\omega t - kR)] \tag{33}$$

If $\boldsymbol{X} = 0$ and the surface is taken to be spherical, the functions $F_1(\boldsymbol{x})$ and $F_2(\boldsymbol{x})$ are defined for a dipole source as

$$F_1(\boldsymbol{x}) = -\int_0^{2\pi}\int_0^{\pi} \frac{n_i l_i}{4\pi r a}[(k^2a^2 - 2)\cos k(r + a) - 2ka\sin k(r + a)]\sin\gamma \, d\gamma \, d\alpha \tag{34a}$$

$$F_2(\boldsymbol{x}) = -\int_0^{2\pi}\int_0^{\pi} \frac{n_i l_i}{4\pi r a}[(k^2a^2 - 2)\sin k(r + a) + 2ka\cos k(r + a)]\sin\gamma \, d\gamma \, d\alpha \tag{34b}$$

When $\boldsymbol{l} = \boldsymbol{e}_3$, then $n_i l_i = \cos\gamma$. When $\boldsymbol{l} = \boldsymbol{e}_1$, then $n_i l_i = \cos\alpha \sin\gamma$.

The Gauss-Legendre stretched subinterval quadrature for double surface integrals as described in Ref. 11 can be applied to calculate the coefficients in the linear system in Eq. (27). The integrals in this linear system are singular when the source point and the observer point coincide. Since the observer point is known, the point of singularity is known. The subintervals in the quadrature are stretched so that more points are concentrated near the singular point, allowing a more accurate and efficient estimate of the integral. If x^* is the singular point, then $\xi^* = (x^* - a)/(b - a)$. Here ξ^* is the transformed singular point. The stretching function is

$$g(\eta) = \frac{(\eta - \xi^*)^n - (-\xi^*)^n}{(1 - \xi^*)^n - (-\xi^*)^n} \tag{35}$$

where n is an integer. The stretched subintervals are

$$a_j = a + (b - a)\, g\left(\frac{j - 1}{M - 1}\right), \quad j = 1,M \tag{36}$$

where $a_1 = a$ and $a_{M+1} = b$. Once the integration is completed, the linear system can be solved for the coefficients c_i and d_i by Gaussian elimination.

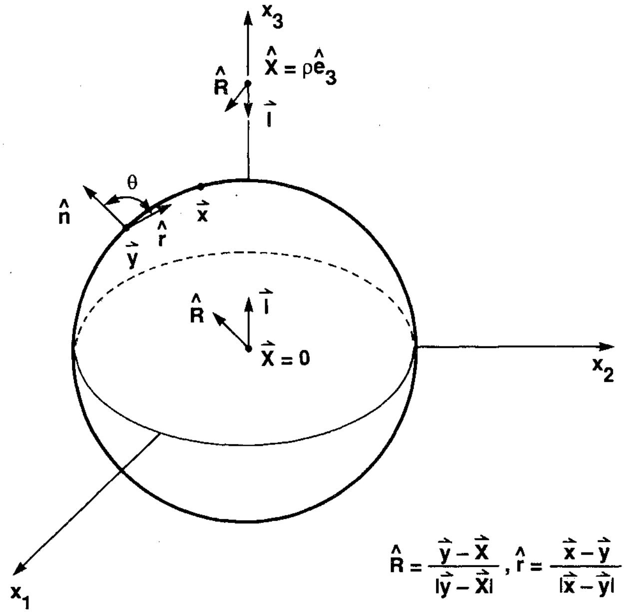

Fig. 1 Geometry for a dipole inside and outside a sphere.

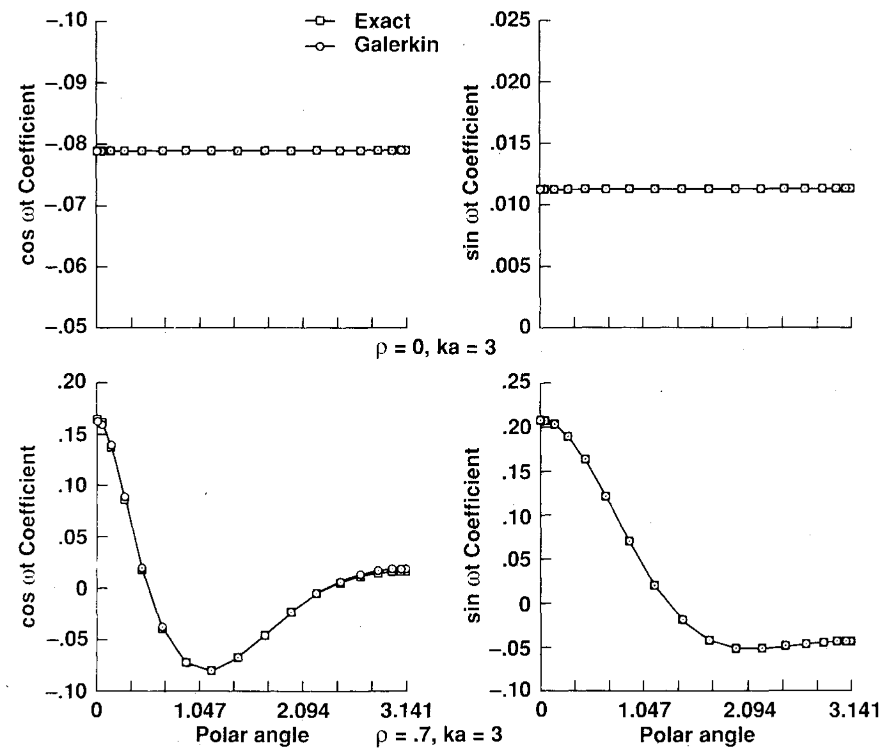

Fig. 2 Comparisons of the Galerkin method solution to the exact solution for monopole pressure fields.

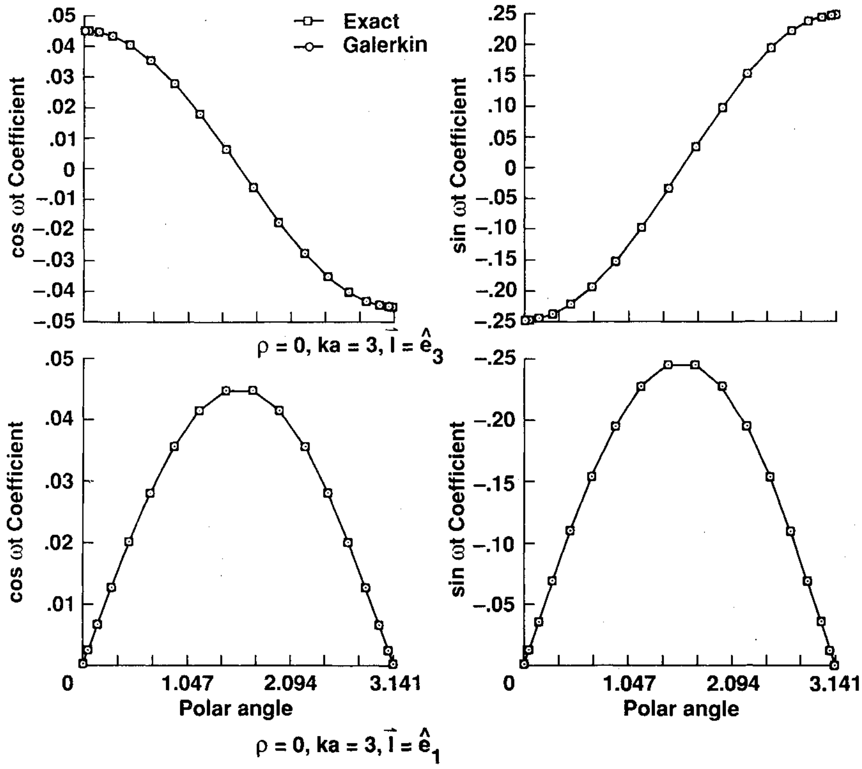

Fig. 3 Comparisons of the Galerkin method solution to the exact solution for dipole pressure fields.

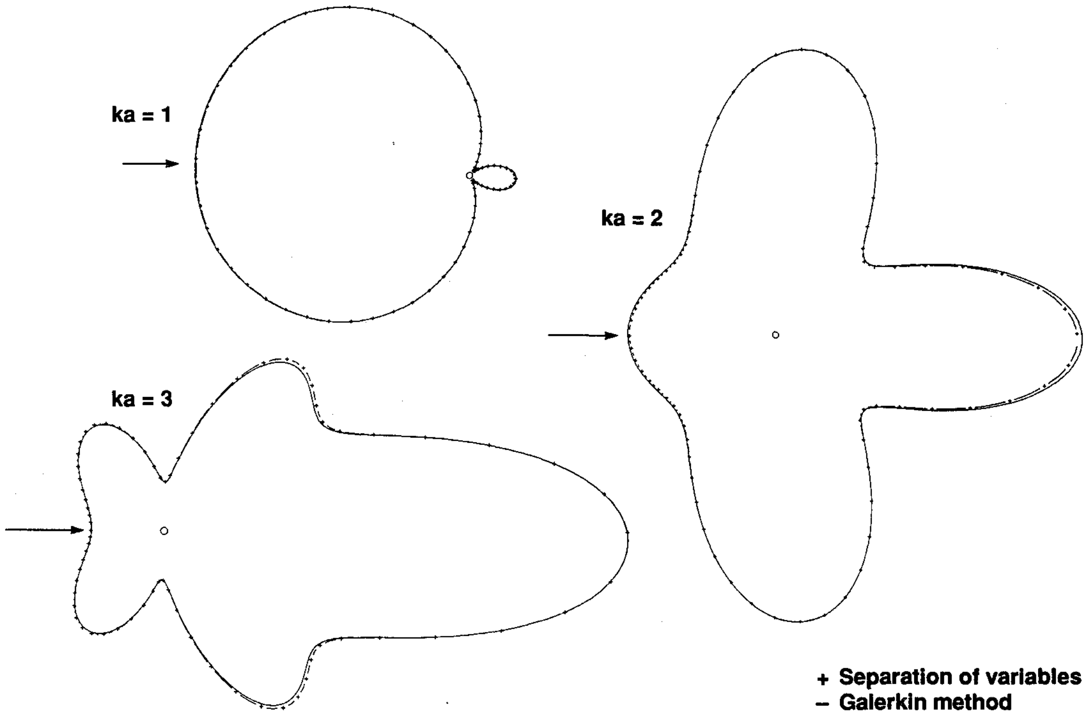

Fig. 4 The directivity patterns for the scattering of plane waves (as approximated by a monopole in the far field) by a rigid sphere, predicted by the Galerkin method, are compared to those derived from the separation-of-variables solution for $ka = 1$, $ka = 2$, and $ka = 3$; ka is the wave number multiplied by the radius of the sphere.

The Galerkin method was first applied to the prediction of the monopole pressure field in the simplest scenario, in which $ka = 3$, $\rho = 0$, and $a = 1$. The second situation tested was for $ka = 3$, $\rho = 0.7$, and $a = 1$. This second situation is a good test of the Galerkin method prediction of the scattered pressure field because the only difference between this second case and the monopole scattering problem is that in the case of the scattering problem, the monopole is outside the sphere. Comparisons of the Galerkin method results to the exact solutions are shown in Fig. 2.

This procedure was also carried out for the dipole pressure field in various situations. The first situation was for $\boldsymbol{l} = \boldsymbol{e}_3$, with $ka = 3$. The second situation was for $\boldsymbol{l} = \boldsymbol{e}_1$, with $ka = 3$. This situation provided a test using more complicated basis functions. Comparisons of the test results to the exact solutions are shown in Fig. 3.

This method can handle higher frequencies, but since more integration points are needed in the estimation of the singular integrals, a considerable amount of time is needed for the solution at higher frequencies.[11] It should be noted, however, that once the surface pressure is known, very little additional computational effort is needed to predict the pressure at any point in the field $f > 0$. The degree of accuracy seen in these solutions by the Galerkin method leads to the assumption that the scattered surface pressure resulting from point monopole or dipole fields can be predicted as accurately by the same technique.

Scattered Pressure Field Solutions

In this section, the Galerkin method is applied to predict the scattered pressure field from a point source incident on a rigid sphere from the sphere's exterior. The first case of interest is the point monopole field incident on a rigid sphere of radius a centered at the origin. If in this case the monopole is in the far field, the incident waves are essentially planar in the vicinity of the scattering sphere. The results of the Galerkin solution for the monopole in the far field can then be compared to those obtained by the separation-of-variables solution for the scattering of plane waves by a rigid sphere, which is discussed by Morse in Ref. 3. This constitutes yet another test of the current formulation and also leads to some results that cannot be obtained simply from the tabulated values in Ref. 3.

The other cases of interest are the scattering of a dipole located either in the near or far field on the x_3 axis with an orientation either parallel to or perpendicular to the x_3 axis.

Scattering of Plane Waves

Since Morse defined the plane wave to be moving in along the x_3 axis, the monopole is also located on the x_3 axis, at a distance far enough away from the sphere that the wave fronts are planar by the time they reach the sphere. If this distance is designated as ρ, the monopole location is $x = \rho e_3$. The functions $F_1(x)$ and $F_2(x)$ for the scattering case are defined exactly as in Eqs. (30a) and (30b) except that they are of the opposite sign and $\rho > a$. The same basis functions are used in the solution of the scattered pressure field as were used in the solution of the monopole field, and the system is solved for the coefficients c_i and d_i in precisely the same way. Therefore all the accuracy should be maintained. The scattered surface pressure solution can then be used in Kirchhoff's representation to predict the scattered pressure at any point in the field. The scattered pressure in the far field is

$$
\begin{aligned}
4\pi\hat{P}_s(x,t) &= \int_{f=0} \frac{1}{r}\frac{\partial}{\partial n} p_m(y,\tau^*)\mathrm{d}S \\
&+ \int_{f=0} \frac{\cos\theta}{r^2} \sum_{i=1}^{N} [c_i\Psi_i(y)(\cos\omega\tau^* - kr\sin\omega\tau^*) \\
&+ d_i\Psi_i(y)(\sin\omega\tau^* + kr\cos\omega\tau^*)]\mathrm{d}S
\end{aligned}
\tag{37}
$$

The directivity patterns obtained by numerically evaluating the scattered intensity from the analytical solution presented by Morse in Eq. (29.10) on page 354, Ref. 3 can be compared to the directivity patterns predicted by the method of Galerkin solution in Eq. (37). This comparison is shown in Fig. (4) for $ka = 1$, $ka = 2$, and $ka = 3$ and in Fig. (5) for $ka = 4$ and $ka = 5$. It is evident that the results shown for the Galerkin method solution match to a very high degree of accuracy the results presented by Morse for $ka = 1, 2, 3, 4$. However, when $ka = 5$ the patterns differ. This difference occurs simply because not enough terms were included in the numerical evaluation of Eq. (29.10); only the first 10 phase angles were tabulated by Morse in Table XI on page 450 in Ref. 3. For the current purpose, it is not useful to perform the fairly involved analysis necessary to extend the tables. It is found that, in the present situation, the Galerkin solution converges faster at higher frequencies than does the separation of variables solution. The directivity patterns at $ka = 6, 7, 8, 9, 10$ are shown in Fig. (18) of Ref. 11.

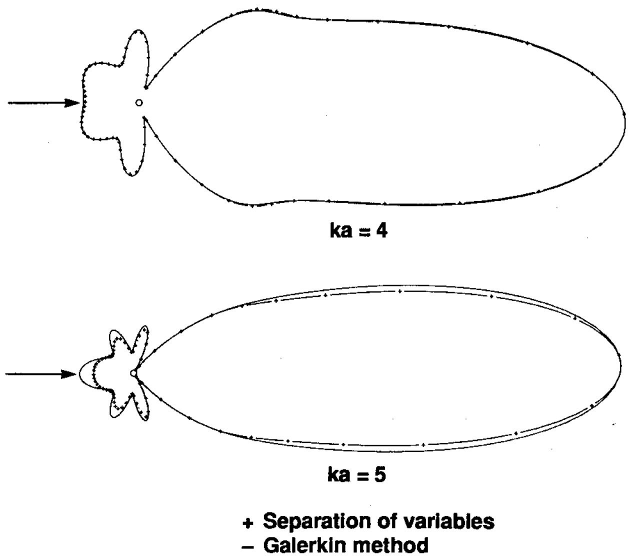

Fig. 5 The directivity patterns for the scattering of plane waves by a rigid sphere, predicted by the Galerkin method, are compared to those derived from the separation-of-variables solution for $ka = 4$ and $ka = 5$.

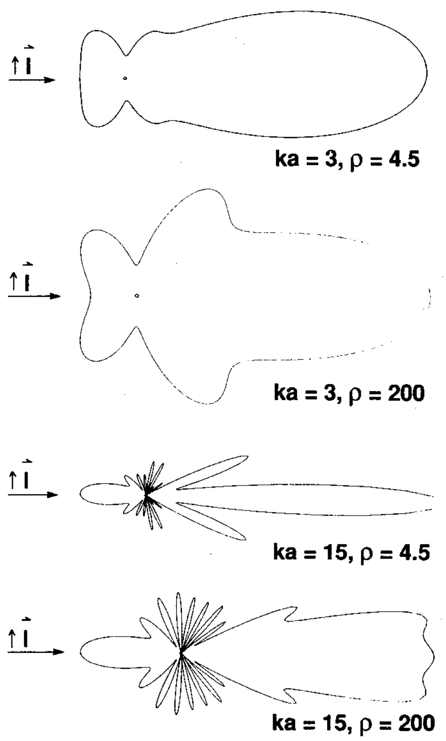

Fig. 6 The directivity patterns for the scattering of a point dipole with $l = e_3$ by a rigid sphere of radius $a = 1$ is plotted as a function of the polar angle for $ka = 3$ and $ka = 15$ in the near field ($\rho = 4.5$) and in the far field ($\rho = 200$).

Scattering of Nonplanar Waves

Given the results illustrated in Figs. 4 and 5, it is reasonable to conclude that the method presented in the current work will be successful in predicting the scattering of nonplanar incident wave fields. The functions $F_1(x)$ and $F_2(x)$ for the dipole located on the x_3 axis a distance ρ from the origin are

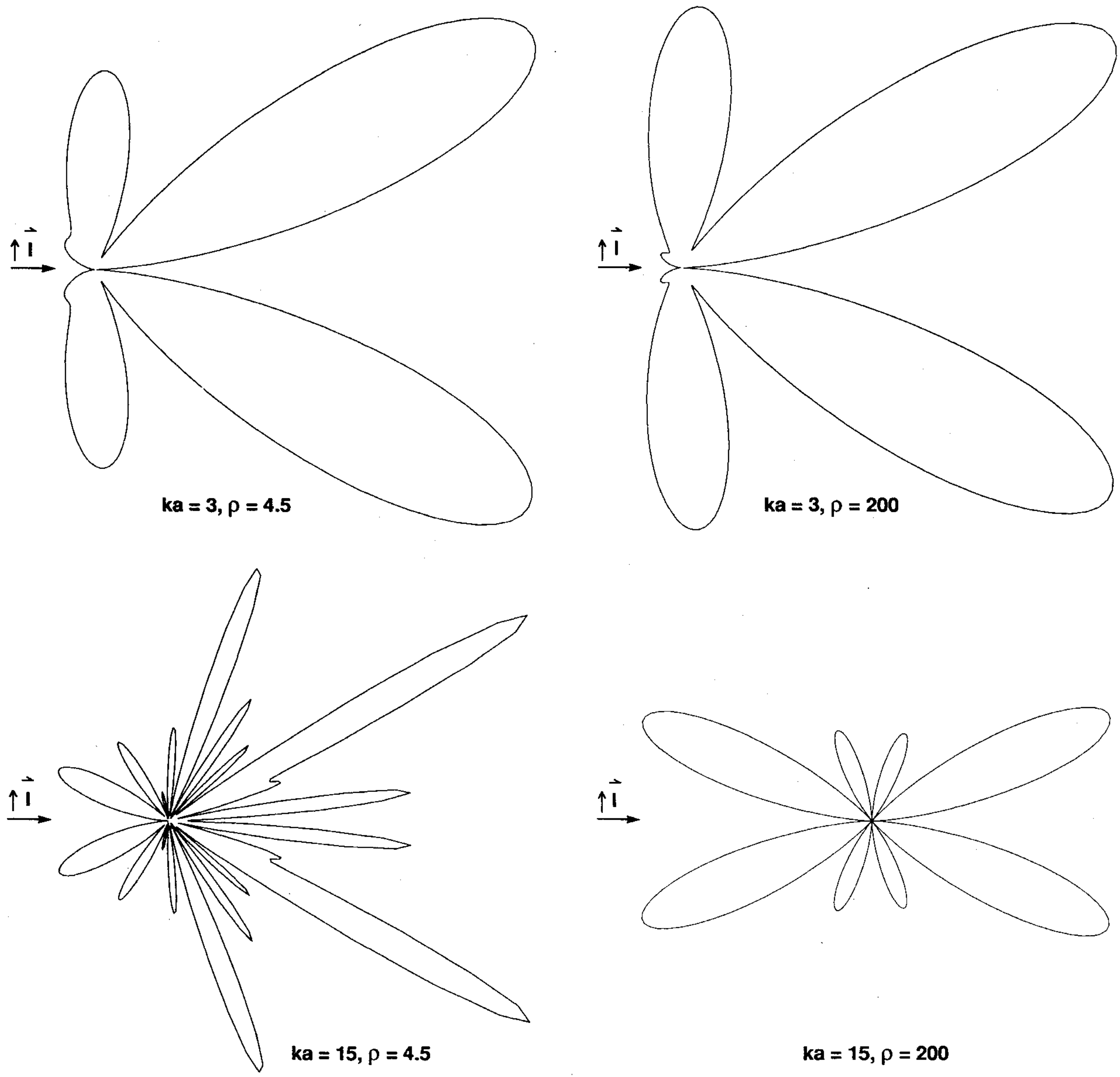

Fig. 7 The directivity patterns for the scattering of a point dipole with $l = e_1$ by a rigid sphere of radius $a = 1$ is plotted as a function of the polar angle for $ka = 3$ and $ka = 15$ in the near field ($\rho = 4.5$) and in the far field ($\rho = 200$).

$$F_1(x) = \int_0^{2\pi}\int_0^{\pi} \frac{1}{4\pi r R^3}\left\{\frac{(a-\rho\cos\gamma)}{R} l_i\hat{R}_i \times [(k^2R^2-3)\cos k(r+R) - 3kR\sin k(r+R)] + n_i l_i[kR\sin k(r+R) + \cos k(r+R)]\right\} a^2 \sin\gamma \, d\gamma \, d\alpha \tag{38a}$$

$$F_2(x) = \int_0^{2\pi}\int_0^{\pi} \frac{1}{4\pi r R^3}\left\{\frac{(a-\rho\cos\gamma)}{R} l_i\hat{R}_i \times [(k^2R^2-3)\sin k(r+R) + 3kR\cos k(r+R)] - n_i l_i[kR\cos k(r+R) - \sin k(r+R)]\right\} a^2 \sin\gamma \, d\gamma \, d\alpha \tag{38b}$$

When $l = e_3$, then $l_i\hat{R}_i = (\alpha\cos\gamma - \rho)/R$ and $n_i l_i = \cos\gamma$. When $l = e_1$, then $l_i\hat{R}_i = (\alpha \sin\gamma \cos\alpha)/R$ and $n_i l_i = a \sin\gamma \cos\alpha$.

The scattered pressure for each dipole orientation is found by first solving the linear system in Eq. (26) for the coefficients c_i and d_i with the $F_1(x)$ and the $F_2(x)$ that are defined in Eqs. (38a) and (38b). These coefficients are then used in Eq. (28) to find the scattered pressure at any point in the field.

Figure 6 shows the directivity of the scattered pressure intensity for the dipole with $l = e_3$ incident on the rigid sphere. The observer is in the far field. The figure shows two cases, one in which the source is in the near field at $\rho = 4.5$, and one in which the source is in the far field at $\rho = 200$. Two frequencies are shown for each case, a low frequency of $ka = 3$ and a high frequency of $ka = 15$. Note that at $ka = 3$ with the source in the far field, the directivity pattern is the same as that for the plane wave previously discussed. This is a result of the fact that this orientation of the dipole causes its maximum intensity to be along the polar axis of the sphere. Figure 7 shows the scattered intensity for the dipole with $l = e_1$ in the same situations as the dipole with $l = e_3$.

Conclusions

A boundary integral approach was applied to the scattering of nonplanar waves by rigid bodies. This approach was proven to be successful through the test of the Galerkin solution of the Kirchhoff representation for point sources. Also, the agreement between the scattered pressure obtained via the Galerkin method solution and the separation-of-variables solution for the scattering of plane waves by a rigid sphere, shown in Fig. 4, is strong evidence that the Galerkin method is capable of solving the boundary integral equation which predicts the scattering of nonplanar waves by rigid spheres. This work presents one of the few solutions for scattering of nonplanar waves and offers some insight on how to solve for the scattering of acoustic fields that can be modeled by point-source pressure fields. In addition, the same type of formulation that was used in the current work to derive the Kirchhoff representation for the scattered pressure field can also be applied to moving surfaces using the extended Kirchhoff formula presented in Ref. 7.

There are certain advantages to the Galerkin method solution of the boundary integral equation. The scattering of any incident field that satisfies the wave equation can be determined and the approach is not limited to geometries for which separation of variables applies, or to limiting cases of high or low frequencies. However, as in the current work, when the scattering obstacle has a simple geometry to which separation of variable applies, the Galerkin method will converge quite quickly if the eigenfunctions are taken as the basis functions. For more complicated scattering geometries, the basis functions will not be a simple set of eigenfunctions and the convergence cannot be expected to be as rapid.

There is an important consequence of using the Kirchhoff formulation as expressed by Eq. (13) for scattering problems of the class treated here. This consequence appears to arise because Eq. (13) involves only the scattered pressure and is constructed so that it always predicts undisturbed conditions interior to the surface $f = 0$ (see Eq. (7)). As a result, the current methodology seems to avoid the divergences often encountered in boundary integral acoustic problems when the incident wave frequency coincides with a resonant frequency of the interior region $f < 0$. For both the monopole and dipole test cases described here, it was found repeatedly that solutions calculated at the characteristic frequencies were obtained as accurately as at any other frequency.[11]

References

[1]Shaw, R. P., "Boundary Integral Equation Methods Applied to Wave Problems," *Developments in Boundary Element Methods—1*, Applied Science Publishers Ltd., London, 1979, pp. 121–153.

[2]Shaw, R. P., "Singularities in Acoustic Pulse Scattering by Free-Surface Obstacles with Sharp Corners," *Journal of Applied Mechanics*, Vol. 38, June 1971, pp. 526–528.

[3]Morse, P. M., *Vibration and Sound*, American Society of Physics, 1976, pp. 346–357.

[4]Shaw, R. P., "Diffraction of Waves by Circular Obstacles with Variable Impedence Boundary Conditions," *Journal of Sound and Vibration*, Vol. 38, No. 4, 1975, pp. 417–424.

[5]Goldstein, M. E., *Aeroacoustics*, McGraw-Hill, New York, 1976, pp. 28–37.

[6]Wardle, L. J., "The Direct Boundary Integral Method for Potential Theory and Elasticity," *The Application and Numerical Solution of Integral Equations,* Sijthoff and Noordhoff. Alphen aan den Rijin, The Netherlands, 1980, pp. 135–148.

[7]Farassat, F., and Myers, M. K., "Extension of Kirchhoff's Formula to Radiation from Moving Surfaces," *Journal of Sound and Vibration*, Vol. 123, No. 3, 1989, pp. 451–460.

[8]Gel'fand, I. M., and Shilov, G. E., *Generalized Functions, Vol. 1: Properties and Operations*, Academic Press, New York, 1964.

[9]Kanwal, R. P., *Generalized Functions—Theory and Technique*, Academic Press, New York, 1983.

[10]Farassat, F., "Discontinuities in Aerodynamics and Aeroacoustics: The Concept and Applications of Generalized Derivatives," *Journal of Sound and Vibration*, Vol. 55, No. 2, pp. 165–193.

[11]Hoeffner, J. M., "A Boundary Integral Approach to the Scattering of Nonplanar Acoustic Waves by Rigid Bodies," M. S. Thesis, George Washington Univ., Washington, DC, Aug. 1988.

[12]Hildebrand, F. B., *Methods of Applied Mathematics*, Prentice-Hall, Englewood Cliffs, NJ, 1965, pp. 278–292.

[13]Schied, F., *Schaum's Outline of Theory and Problems of Numerical Analysis*, McGraw-Hill, New York, 1968, pp. 125–139.